Consistent digital color image acquisition of the skin

Yves Vander Haeghen*,***, Prof. Dr. J.M. Naeyeart**, Prof. Dr. I. Lemahieu*
* Dept. Engineering, ELIS-MEDISIP, University Gent, St.-Pietersnieuwstraat 41, 9000 Gent, Belgium
** Dept. Dermatology, University Hospital, De Pintelaan 185, 9000 Gent, Belgium
***E-mail: Yves.VanderHaeghen@rug.ac.be

Abstract— **We propose a simple, quick and practical color calibration procedure that results in a precise (reproducible), albeit not very accurate (close to values obtained with a reference device), color description in a standard device-dependent color space (sRGB). The system consists of a 3-chip CCD camera, a continuous ring-light, frame grabber and PC. The calibration procedure involves building a profile of the acquisition system based on 24 color targets with known characteristics. This profile is easily checked before a set of image acquisitions and remains valid for a long period. The acquired images are transformed from the device-dependent RGB camera space to the gamma corrected sRGB (or ITU-R BT.709) space and are readily displayable on a CRT-based monitor. Moreover, sRGB tristimulus values are readily transformed to the CIE L*a*b* space, allowing perceptual color differences (ΔE^*_{ab}) to be computed. Although the accuracy of the proposed procedure is not very high ($\Delta E^*_{ab} > 10$ for some of the color targets), the precision or reproducibility is quite good. The short-term precision based on 20 consecutive measurements of a white patch is $\langle \Delta E^*_{ab} \rangle = 0.04$, with $\Delta E^*_{ab} < 0.1$. The medium-term precision, based on 10 measurements of the 24 color patches made during different warm-up cycles of the acquisition system under one profile is $\langle \Delta E^*_{ab} \rangle = 0.34$, with $\Delta E^*_{ab} < 1.2$. Long-term or inter-profile precision is of the same order, even when the color temperature of the light source is changed between profiles.**

Keywords— **Color calibration, Dermatology, Color image acquisition, camera calibration, CCD camera**

I. Introduction

In dermatology color and color difference often convey important diagnostic information, especially when investigating pigmented lesions and more particularly skin cancer. In order to make quantitative color measurements on irregular and variable sized skin lesions, standard chromameters or spectrophotometers are generally useless because of their fixed aperture. Traditional photography has the benefit of having a visual record of the lesion, but doesn't have very consistent color reproduction due to differences in film, illumination and development. Although in digital photography no film is involved, it not straightforward to obtain a constant response from a digital image acquisition system [1], [2]. Moreover, most digital cameras are not colorimetric, i.e. their color sensors don't have spectral response functions that are proportional to the CIE $\bar{x}\,\bar{y}\,\bar{z}$ color matching functions (CIE stands for 'Commission Internationale de l'Eclairage', a standardizing body in the field of color science). This means it is not easy to compute perceptual color differences because the relation between the device-dependent camera RGB space and the device-independent CIE XYZ space is unknown and has to be determined. This subject was already extensively covered in the literature [3], [4], [2], [5], [6], [7], [8], [9], but here the emphasis is clearly on a simple and practical scheme, making no pretense at being a color appearance model or at color constancy. Instead it avoids some of the problems concerning changes in illuminant between source (camera RGB) and output space (sRGB). The use of digital photography in dermatology has already been investigated several times, mostly using device-dependent color spaces, e.g. RGB and HSV [10], [11], [12], [13]. Sometimes device-independent color spaces were used [14], although it is unclear just how the necessary transform was obtained. At present no system for use in dermatology has been proposed that uses a standard color space with known primaries and white point. Such a color space has the additional benefit of allowing the interchange of images for more than just viewing purposes, and opens perspectives in the area of telemedicine.

II. The acquisition system

The acquisition system consists of a JVC KY-55B 3-chip CCD camera with a Pentax manual zoom lens, a Schott[1] KL1500 150 Watt halogen light source and an Integral Technologies[2], FlashPoint 128 frame grabber. The field of view of the CCD camera is 2.0 cm by 1.5 cm. With an image containing 760 by 570 pixels the resolution is 38 pixels/mm. The light source is linked by a 2 m long optical fiber to a continuous ring-light that fits around the zoom lens. A blue filter changes the color temperature of the light source from 2800 K to around 5100 K, making it a rough approximation of a CIE D50 illuminant. The frame grabber is fitted in a standard 150 MHz Pentium

[1] Shott Glaswerke, Hagenauer strasze 38, D-65203 Wiesbaden
[2] Integral Technologies, Inc, 9855 Crosspoint blvd, Suite 126, Indianapolis, Indiana, 46256 USA

PC running Windows 95, and acquisition is done using the PAL analog RGB format which is digitized with 8-bit precision per color channel. The settings of the CCD camera can be adjusted through the serial port of the PC. The settings of the frame grabber are controlled using the FlashPoint Software Developer's Toolkit 3.0 from Integral Technologies. The color targets are taken from the MacBeth Color Checker Chart[3] (MBCCC).

III. Determining the acquisition system profile

The calibration of the whole acquisition system consists of several consecutive steps: determination of the camera offset, the frame grabber offset, the frame grabber gain, the camera aperture, the color gains of the camera, the linearizing look-up table, and finally the transform from the device-dependent RGB space to the device-independent CIE XYZ space. All these settings are stored in a so-called profile of the acquisition system. Before discussing each of these steps the simple camera and frame grabber models upon which they are based are reviewed.

A. The camera and frame grabber model

The output voltage V_c^{cam} of the camera for a certain color channel $c = R, G, B$ and for a certain pixel i can be written as:

$$V_{c,i}^{cam} = \Psi_0^{V_{max}^{cam}} \left([V_{offset}^{cam} + g_c^{cam}(V_{c,i}^{CCD} + V_{dark}^{CCD})]^{0.45} \right) \tag{1}$$

with V_{offset}^{cam} a variable offset voltage, $V_{c,i}^{CCD}$ a voltage proportional to the light incident on the element corresponding with the same pixel in the CCD array of color channel c, and V_{dark}^{CCD} the voltage resulting from the very temperature sensitive CCD dark current; g_c^{cam} is a variable color channel dependent gain, which is always 1 for the green channel. This is the reason the green channel will always be used in determining color channel independent parameters. The function $\Psi_0^{V_{max}^{cam}}$ represents the clipping that occurs when an output voltage is out of range:

$$\Psi_0^{V_{max}}(V) = \begin{cases} 0 & \text{if } V < 0 \\ V & \text{if } 0 \leq V \leq V_{max} \\ V_{max} & \text{if } V > V_{max} \end{cases} \tag{2}$$

The 0.45 power dependence is called the gamma correction, and is a correction for the way a CRT-based display works. This feature can be turned off, but due to a similar non-linearity of the human visual system (HVS), it is better to digitize gamma corrected RGB values (R*G*B*), and apply the inverse operation before any further processing [15]. The 8-bit digitized R*G*B* pixel value P_c^* of the frame grabber and the linear RGB pixel value P_c may be written as:

$$\begin{aligned} P_c^* &= \Re \left(255 \left[\frac{\Psi_0^{V_{max}^{fg}}(V_{offset}^{fg} + g^{fg} V_c^{cam})}{V_{max}^{fg}} \right] \right) \\ P_c &= \left[\frac{P_c^*}{255} \right]^{2.2}, P_c \in [0\ 1.0] \end{aligned} \tag{3}$$

with V_{offset}^{fg} again a variable offset voltage, g^{fg} the variable frame grabber gain and $\Re$ the integer rounding operator.

In reality (1) and (3) depend on more variable parameters, but these are not relevant to the proposed scheme. The camera parameters V_{offset}^{cam} and g_c^{cam} can be set using values in the range [0, 255], while the frame grabber values for V_{offset}^{fg} and g^{fg} have to be in the range [0, 63]. The relationship between these values and the variable parameters is linear.

B. The camera offset voltage

The aim is to make sure that a totally non-reflecting target, i.e. a target with reflective luminance $Y = 0$, results in $V_G^{cam} = 0$. Turning the light source off, closing the lens diaphragm and putting the lens cap on provides us with such a target. As no other parameters of the acquisition system have been properly set so far we cannot determine an aim pixel value P_G^* or P_G for the target. We therefore adopt the following scheme:

1. Make sure the target produces a non-zero image averaged green pixel value $\langle P_G \rangle$ by setting a high frame grabber gain and offset.
2. Measure $\langle P_G \rangle$ in function of the camera offset voltage parameter.

It can be seen using (1) and (3) that this will result in a curve consisting of two straight lines: one horizontal line as long as $V_{offset}^{cam} \leq -g_c^{cam} V_{dark}^{CCD}$, and one sloping line once clipping no longer occurs and $V_{offset}^{cam} \geq -V_{dark}^{CCD}$ (see fig. 1). At the setting at which the two lines intersect the offset voltage exactly compensates for the voltage resulting from the dark current, and $V_G^{cam} = 0$. To determine this point reliably and independently of the frame grabber settings we fit a horizontal and a sloping straight intersecting at each of the offset voltage settings through the data, and compute the fitting errors. The desired setting is the one with the lowest error (see fig. 1). We will refer to this operation as the two-line intersection method.

C. The frame grabber offset voltage

Next we determine the setting of the frame grabber offset voltage so that $\langle P_G^* \rangle = \langle P_G \rangle = 0$. Because $V_G^{cam} = 0$ for the $Y = 0$ target, $\langle P_G^* \rangle$ is independent of the frame grabber gain g^{fg}. This means theoretically we only have to find the highest offset voltage setting at which $\langle P_G^* \rangle$ is zero. However, we still favor the two-line intersection

[3] Macbeth, 405 Little Britain rd, New Windsor, NY 12553-6148, USA

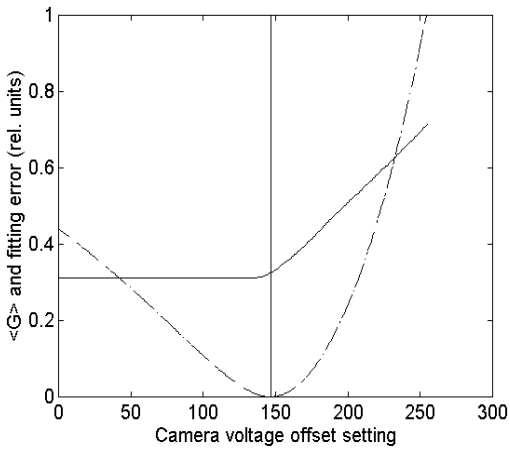

Fig. 1. The image averaged linear pixel value for the green channel in function of the camera voltage offset setting (solid line) and the corresponding fitting errors (dashed line). The setting with the smallest fitting error is indicated by the vertical solid line. $\langle G \rangle$ actually denotes $\langle P_G \rangle$.

method as being more robust and general. It is important to note that because the camera signal V_G^{cam} doesn't change but is digitized with another offset voltage only P_G^* has a piecewise linear relationship with the offset voltage, and not P_G!

D. The frame grabber gain and camera lens aperture

In order to maximize the dynamic range of the camera we wish that $\langle P_G^* \rangle = 255$ for a perfectly reflecting target ($Y = 100$), given the light source. This can be achieved in two steps. First g^{fg} is set so that the maximal camera signal V_{max}^{cam} is digitized as 255. For this the camera CCD's are saturated by fully opening the lens aperture, and measuring the highly reflecting MBCCC 'white' target ($Y = 90$). Then $\langle P_G \rangle$ is measured in function of g^{fg} and the two-line intersection method is again used to determine the optimal gain setting. Secondly, the continuous aperture of the lens is adjusted manually until $< P_G^* >= 255\left[\frac{90}{100}\right]^{0.45} = 242.2$ for the same 'white' target.

E. The camera color balance and linearizing look-up table

The aim of these two operations is to obtain a linear response from the acquisition system for series of color targets with the same chromaticity coordinates $\frac{X}{X+Y+Z}$ and $\frac{Y}{X+Y+Z}$, but different luminance Y: $P_R \sim Y$, $P_G \sim Y$ and $P_B \sim Y$. When using color targets with an almost constant reflectivity in function of wavelength (e.g. 'neutral' colors of the MBCCC), and with the added desire to optimize the dynamic range of each color channel separately for the given light source, this becomes $P_R = P_G = P_B = Y/100$ (graybalancing). This process is actually a kind of normalization of RGB values with regard to the light source.

Practically the camera color dependent gain factors g_R^{cam} and g_B^{cam} are adjusted first so that graybalance is obtained for the MBCCC 'white' target using a simple bisection root finding method. Hereafter the lookup-table (LUT) is constructed in order to achieve graybalance for the 5 other MBCCC 'neutral' color targets with luminance ranging from 3.1 to 59.1.

F. The RGB to CIE XYZ transform

Assuming that the CIE $\bar{x}\,\bar{y}\,\bar{z}$ color matching functions can be written as linear combinations of the camera RGB primaries, the relationship between RGB and XYZ tristimuli under the same unknown camera illuminant is also linear. If this camera illuminant is not too different from the D65 illuminant of the sRGB space, then XYZ tristimuli under the camera illuminant can be approximately computed from their D65 counterparts with a linear transform [9]. This means that under the above mentioned conditions we can map the camera RGB tristimuli of the MBCCC targets to their D65 XYZ tristimuli using a linear transform T. Currently the XYZ tristimuli are white-point normalized which means that T operates between equal ranges of [0.01.0]. The transform T was computed using singular value decomposition, which actually gives a least-squares solution for an overdetermined system of linear equations. It is clear that minimizing the mapping errors in a more perceptual color space, e.g. R*G*B* or CIE L*a*b*, would be far better, but this means tackling non-linear optimization in a multidimensional space. The white-point preserving transformation proposed in [6] performs very well, especially under maximum ignorance assumptions. However, as the proportion of neutral color targets used in determining T is quite large there will be a 'natural' bias in the least-squares procedure towards properly mapping neutral colors. Moreover, the maximum ignorance assumption may not be the best premise in the case of skin imaging.

IV. Checking and adjusting an existing acquisition system profile

Once a profile is determined and stored it can be used as long as the acquisition system doesn't change too much (aging of the light source bulb, changes in CCD sensor spectral response, ...). This is easily checked by comparing the CIE L*a*b* value of a test target (MBCCC 'white') with its value during the calibration procedure. We set a limit of $1\,\Delta E_{ab}^*$ unit as the maximum deviation for the acceptance of the profile. Of more concern is the changing response of the acquisition system in function of the warmup-time (see fig. 3): even though the system more or less stabilizes after 30 minutes, the blue response continues to change and diverges from the red and green response. The profile used here was determined after a warmup-time of around 60 minutes. It is clear an increasing difference between the calibration and the mea-

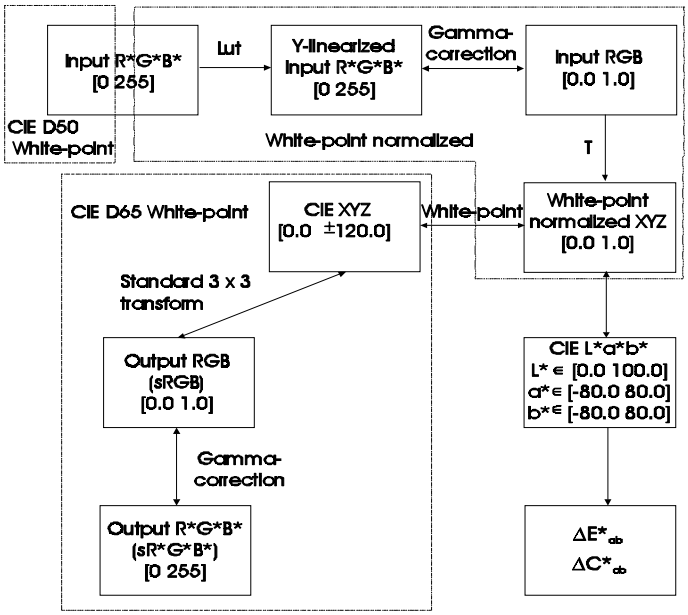

Fig. 2. The different color spaces of the calibration scheme and their relations.

surement time results in an increasing error, even though these remain generally small enough for the acceptance of the profile. Assuming that the non-linearity of the acquisition system doesn't change with slight changes in the frame grabber gain g^{fg} and camera color dependent gains g_R^{cam} and g_B^{cam}, i.e. assuming the linearizing LUT and the transform T remain valid, we can adjust these parameters on the fly when checking a profile. This doesn't involve any extra interaction as the same test target is used, and markedly improves the precision. Images acquired with

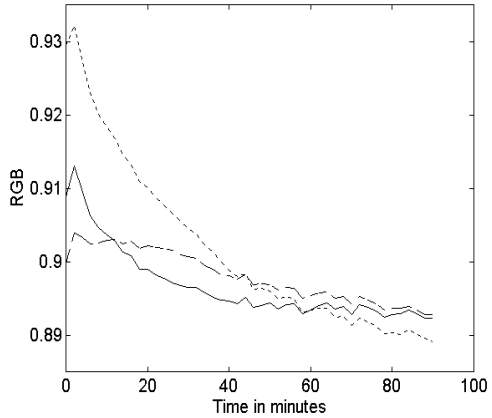

Fig. 3. The R (solid line), G (dashed line) and B (dotted line) response of the white MBCCC target in function of the warmup-time.

a validated and adjusted profile are transformed to the gamma corrected sRGB space before they are stored, see fig. 2 This is called output rendering and should provide a fairly realistic image on any modern CRT-based monitor which has its white-point set at 6500 K [16].

V. Experimental results and discussion

With accuracy we mean the consistency with which measurements of colors are close their real measured values, as measured by a reference instrument, e.g. a spectrophotometer. Good accuracy will be especially important when exchanging images. Experiments consisted of 19 measurements of the MBCCC targets under different profiles and after different warmup-times. For each target t the average error $\langle \Delta E^*_{ab}(t) \rangle$ was computed with regard to the real CIE L*a*b* value of the target, see fig. 4. Two conclusions present themselves: firstly, the RGB to CIE XYZ transform does indeed perform well for neutral colors (targets 19 to 24), and secondly, the greatly varying results between the targets indicates that, as expected, the minimization of mapping errors in the CIE XYZ space is not such a good idea. Averaged over all the MBCCC targets we get $\langle \Delta E^*_{ab} \rangle = 4.1$ with $\Delta E^*_{ab} < 12$. It has to be noted that proper accuracy measurements should use other targets than the ones used in the determination of the acquisition system profile. Real accuracy may therefore be lower than presented here.

With precision we describe the reproducibility of

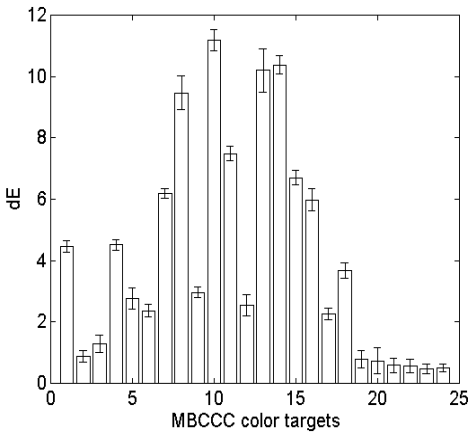

Fig. 4. The average accuracy of the MBCCC color targets. The error bars represent one sample standard deviation

measurements, or the way repeated measurements are spreaded around the average of those measurements. Precision will be important for any quantitative measurement of image color characteristics. We can distinguish several types of precision: short-term precision when making several consecutive measurements of the same target, medium-term or profile precision when comparing measurements made under one profile, and long-term or inter-profile precision when talking about the agreement between measurements made under different profiles.

Short term precision based on 20 consecutive measure-

ments of the MBCCC 'white' target was very good: $\langle \Delta E^*_{ab}(white) \rangle = 0.04$, with $\Delta E^*_{ab}(white) < 0.1$. The results for the medium-term and long-term precision can be seen in fig. 5 and 6. Here the average error $\langle \Delta E^*_{ab}(t) \rangle$ for each target was computed with regard to the average sample CIE L*a*b* value of the target (10 and 9 measurements respectively). To simulate possible long-term changes in the acquisition system, the color temperature of the light source was modified for half of the profiles of fig. 6. There was no noticeable difference in precision between profiles for the normal and modified acquisition system. The average, standard deviation and maximal errors over all the MBCCC targets for medium-term and long-term precision are $\langle \Delta E^*_{ab} \rangle = 0.34$, $s = 0.094$ with $\Delta E^*_{ab} < 1.2$, and $\langle \Delta E^*_{ab} \rangle = 0.30$, $s = 0.10$ with $\Delta E^*_{ab} < 1.2$ respectively. The fact that the long-term precision is slightly better than the medium-term precision might be explained by the fact that any measurements for the long-term precision were made directly after the profile was determined, thereby avoiding the drift problems outlined in fig. 3.

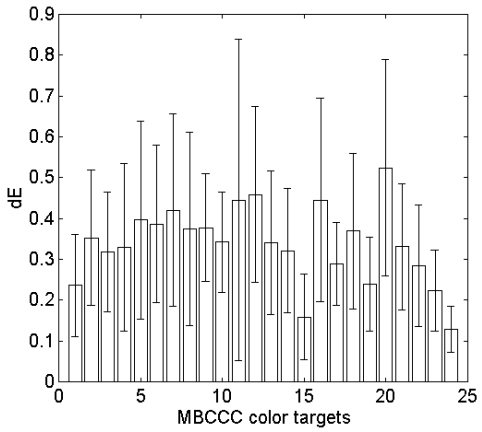

Fig. 5. The average ΔE of the MBCCC color targets under one profile. The error bars represent one standard deviation

VI. Conclusions

We have proposed a color calibration procedure which allows colorimetrically consistent acquisition of digital images. These images are stored in a standard color space with known primaries and white-point, and as such can be exchanged and compaired with other images in the same color space, even if acquired by other means. They are readily displayable on CRT-based displays. The current system is optimized for the acquisition of small field-of-view skin images, and will at first be used in a study of pigmented skin lesions, but it can be useful in any study of natural or induced physiological manifestations in the skin (drug testing, cosmetics, UV-radiation studies, ...).

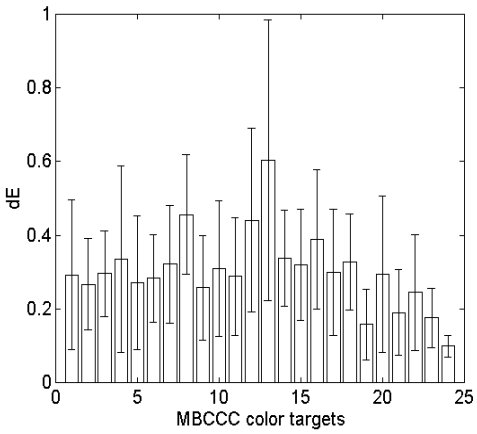

Fig. 6. The average ΔE of the MBCCC color targets under different profiles. The error bars represent one standard deviation

VII. Acknowledgment

This project is funded by the FWO in Belgium, ref. F7801

References

[1] G. E. Healey and R. Kondepudy, "Radiometric CCD camera calibration and noise estimation," *IEEE Transcations on Pattern Analysis and Machine Intelligence*, vol. 16, no. 3, pp. 267–276, 1994.

[2] Y.-C. Chang and J. F. Reid, "RGB calibration for color image analysis in machine vision," *IEEE Transactions on Image Processing*, vol. 5, no. 10, pp. 1414–1422, 1996.

[3] B. A. Wandell, "The synthesis and analysis of color images," *IEEE Transactions on Pattern Analysis and Machine Intelligence*, vol. PAMI-9, no. 1, pp. 2–13, 1987.

[4] D. Slater and G. Healey, "The illumination-invariant recognition of 3d objects using local color invariants," *IEEE Transactions on Pattern Analysis and Machine Intelligence*, vol. 18, no. 2, pp. 206–210, 1996.

[5] G. Finlayson, "Color in perspective," *IEEE Transactions on Pattern Analysis and Machine Intelligence*, vol. 18, no. 10, pp. 1034–1038, 1996.

[6] G. D. Finlayson and M. S. Drew, "White-point preserving color correction," in *Fifth Color Imaging Conference: Color Science, Systems and Applications*, pp. 258–261, IS&T, SID,, 1997.

[7] E. Boldrin, P. Campadelli, and R. Schettini, "Learning colkor appearance models," in *Fifth Color Imaging Conference: Color Science, Systems and Applications*, pp. 173–176, IS&T, SID,, 1997.

[8] P. M. Hubel, J. Holm, G. D. Finlayson, and M. S. Drew, "Matrix calculations for digital photography," in *Fifth Color Imaging Conference: Color Science, Systems and Applications*, pp. 105–111, IS&T, SID,, 1997.

[9] H. Kang, *Color Technology for Electronic Imaging Devices*. SPIE Optical Engineering Press, 1997.

[10] N. Cascinelli et al., "A possible tool for clinical diagnosis of melanoma: The computer," *Journal of the American Academy of Dermatology*, vol. 16, no. 2, Part 1, pp. 361–367, 1987.

[11] J. L. Stone, R. L. Peterson, and J. E. Wolf, "Digital imaging techniques in dermatology," *Journal of the American Academy of Dermatology*, no. 5, part 1, pp. 913–917, 1990.

[12] R. Kenet et al., "Clinical diagnosis of pigmented lesions using digital epiluminescence microscopy," *Arch. of Dermatology*, vol. 129, pp. 157–174, 1993.

[13] W. Stolz et al., "Improvement of monitoring of melanocytic skin lesions with the use of a computerized acquisition and surveilland with a skin surface microscopic television camera,"

Journal of the American Academy of Dermatology, vol. 35, no. 2, Part 1, pp. 202–207, 1996.

[14] T. Schindewolf et al., "Evaluation of different image acquisition techniques for a computer vision system in the diagnosis of malignant melanoma," *Journal of the American Academy of Dermatology*, vol. 31, no. 1, pp. 33–41, 1994.

[15] G. Holst, *CCD arrays, Cameras and Displays*. SPIE Optical Engineering Press, 1996.

[16] J. Holm, "Issues relating to the transformation of sensor data into standard color spaces," in *Fifth Color Imaging Conference: Color Science, Systems and Applications*, pp. 290–295, IS&T, SID,, 1997.